

# Corrosion behaviour of fly ash, alumina and hybrid particles reinforced A356 composites

S. G. Kulkarni<sup>a</sup>, J. V. Menghani<sup>b</sup> Achchhe Lal<sup>c</sup>

<sup>a</sup>*Research scholar, Department of Mechanical Engineering, S.V.N.I.T. Surat-395007, India,*  
[swanand29@rediffmail.com](mailto:swanand29@rediffmail.com)

<sup>b,c</sup>*Assistant professor, Department of Mechanical Engineering, S.V.N.I.T. Surat-395007,*

## Abstract

The corrosion behaviour of A356 alloy matrix composites developed with the use of fly ash, alumina and hybrid particulates as reinforcements are investigated. Fly ash and alumina mixed in weight ratios 1:1 are utilized to make hybrid composition. The 4, 8, and 12 weight percent (wt.%) of the reinforcements are used with A356 alloy matrix using stir casting process. Electrochemical impedance spectroscopy (EIS) in the conventional three-electrode configuration is employed to test the composites during their exposure to 3.5 wt. % NaCl aqueous solution. The corrosion mechanism is studied with the aid of scanning electron microscopy. The results show that the composite of 4 and 8 wt. % fly ash reinforcement have superior corrosion resistance as compared to hybrid and alumina reinforcement while corrosion resistance of fly ash reinforced composite drastically found inferior at 12 wt. % reinforcement.

**Keywords:** Corrosion; Electrochemical impedance spectroscopy; Fly ash; A356; Alumina.

## Introduction

The use of aluminium matrix composites (AMCs) in marine, automobile, aerospace, sporting and other related industries is increasing insistently as a result of their better specific strength and modulus. The AMCs have prominence due to their design flexibility. Brake rotors, cylinder liners, engine parts, pistons, cylinder heads, etc. are some application areas where persistent improvement and usage of particulate composites is increasing [1–3]. Additionally, particulate composites exhibit isotropic material properties [4]. The particulate reinforced composites are less expensive than fiber-reinforced composites and are manufactured by conventional methods [5]. Alumina (Al<sub>2</sub>O<sub>3</sub>) and silicon carbide (SiC) are the reinforcement particles normally used in AMCs, but these are expensive to permit their extensive use therefore lower cost reinforcement materials are required to remove this price hurdle [6,7]. The scope in AMCs containing low-cost and low density reinforcements

is increasing [8]. Together with several particulate reinforcements, fly ash is the most economical and lightweight reinforcement and available in huge quantities as industrial waste. Moreover, fly ash has potential to minimize the cost and density, improve the mechanical properties including strength, stiffness, wear resistance, and hardness. It is stated that the wear resistance of Al–Al<sub>2</sub>O<sub>3</sub> and Al–SiC composite is almost similar to Al–fly ash composite [9]. The tensile, compression strength and hardness [10, 11] as well as wear resistance [12] of composite increases with the increase in the wt. % of fly ash reinforcement.

As a result of simplicity and low manufacturing cost, the stir casting method is used in present work for manufacturing A356 alloy matrix composite. Besides, stir casting process can be used for producing intrinsic as well as heavy shape components [13–15].

The hybrid AMCs have revealed better mechanical and wear resistance properties over composites with single reinforcement and these are currently developing for performance optimization [16, 17]. Additionally, hybrid composites have applications in aerospace and automobiles [18]. However, the less information is available on the corrosion resistance performance of fly ash hybrid composites.

Corrosion studies have been conducted on aluminium composites reinforced with graphite, silicon carbide, alumina, boron and mica in the form of particles, fibers, whiskers or monofilaments but literature on the corrosion of aluminium based composites is often contradictory. Variety of aluminium alloy matrix and reinforcement type combinations exhibits completely different corrosion behaviour. As reinforcement volume fraction in matrix increases, number of properties of composite material changes. Reinforcement materials have higher corrosion resistance compared to the matrix materials [19]. However, the literature study shows that, corrosion increases with increase in fly ash content in aluminium [12]. The Al–SiC composite has more corrosion susceptibility in marine (chloride) environments [19]. It has been also reported that Al–alumina composites exhibits better corrosion resistance than monolithic Al alloys in NaCl solution [21]. Corrosion resistance performance of AMCs is recognized to be arduous to broadly predict as wide deviation is shown and controverting results are reported by researchers for different AMCs [22–24].

The estimation of the corrosion behaviour of AMCs in diverse atmospheres is greatly supportive to establish its appropriateness and performance in many service environments. As currently very less amount of data is available to understand corrosion mechanisms, it is prominently essential to study the effect of fly ash as hybrid reinforcements in AMCs developed by low cost stir casting method. Presently, there is less work available on the

corrosion behaviour of A356 alloy matrix composites manufactured under similar conditions besides reinforced with fly ash, alumina and hybrid reinforcements. The attention on this study is important as A356–fly ash, A356–hybrid and A356–alumina composites have enhanced mechanical properties [25]. The outcome from present work will be supportive in understanding the corrosion behaviour of these in frequent AMCs as well as in constructing a databank of material properties for A356–fly ash, A356–alumina and A356–hybrid composites manufactured by stir casting method under similar circumstances.

The aim of the current work is to study the effect of alumina, fly ash and hybrid composition of alumina and fly ash particulate reinforcements in A356 aluminium alloy matrix for corrosion resistance behaviour. Attempts have been made to examine the effect of reinforcement type, reinforcement weight percentage and hybrid composition on corrosion resistance behaviour of manufactured composites. Electrochemical impedance spectroscopy (EIS) in the conventional three-electrode configuration is employed to test the composites during their exposure to 3.5 wt% NaCl aqueous solution. The corrosion mechanism is studied with the aid of scanning electron microscopy. This study will help to evaluate the effectiveness of hybrid composition of fly ash and alumina for proposing the use of composites for corrosion resistance applications to actual use in industries to accomplish the industry's needs.

## Experimental procedure

### Matrix material

Aluminium alloy A356 is popular as a matrix material due to excellent castability, good corrosion resistance, weldability, better machinability and mechanical properties than other alloys. Aircraft pump parts, structures and fittings, water-cooled cylinder blocks are some typical applications of A356 alloy. The composition limits of A356 are given in Table 1.

Table 1 Composition limits of A356.

Name of constituent	Cu max	Mg	Mn max	Si	Fe max	Zn max	Ti max	Other	Al
Percentage	0.25	0.20 to 0.45	0.35	6.5 to 7.5	0.6	0.35	0.25	0.05	Bal

## Reinforcement material

In present work as received fly ash from power plant, alumina and hybrid of fly ash and alumina is used as reinforcement material. Hybrid reinforcement is formed from equal amount of alumina and fly ash. Considerable research has been undertaken for proper utilization of fly ash. Figure 1 shows scanning electron microscopy (SEM) and Table 2 shows energy dispersive spectroscopy (EDS) of fly ash. With energy dispersive spectroscopy content in the fly ash has been found which is essential to know the type of ash and its effect on the properties of manufactured material. Figure 1 shows the cenospheres present in the fly ash which are light in weight. Table 2 indicates that fly ash used in present work consists of 58.28% silica and 32.22 % alumina.

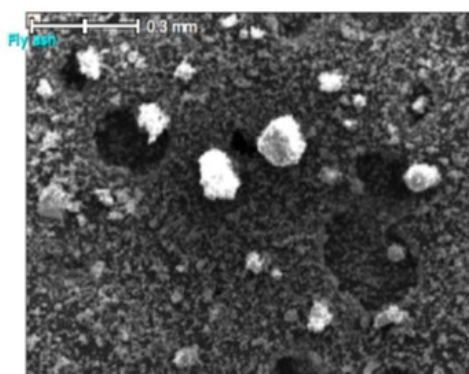


Figure 1. SEM of fly ash.

Table 2 EDS of fly ash

Element	(keV)	mass%	Error%	At%	Compound	mass%	Cation	K
O		48.52						
Al K	1.486	17.05	0.61	22.09	Al <sub>2</sub> O <sub>3</sub>	32.22	5.00	32.6303
Si K	1.739	27.24	0.71	67.81	SiO <sub>2</sub>	58.28	7.68	49.6162
Ca K	3.690	2.24	0.78	3.91	CaO	3.14	0.44	6.0594
Fe K	6.398	4.94	1.53	6.18	FeO	6.36	0.70	11.6942
Total		100.00		100.00		100.00	13.82	

## Fabrication of composite

A356–fly ash, A356–alumina and A356–hybrid composites are produced from stir casting method. An enhanced stir casting process is performed. A356 ingots are cut into small pieces. Washed A356 pieces are kept inside the cast iron crucible. The temperature above the melting point of A356 alloy is maintained in the crucible for uniform melting. Complete melting of A356 alloy is carried. The temperature inside the crucible is raised by 100°C further and is held for 30 minutes to reduce the porosity. Fly ash, alumina and hybrid

reinforcement is added by 4, 8, 12 wt. % in A356 alloy to manufacture a composite. Preheating of reinforcement particle is performed for 400°C to avoid temperature difference between melt A356 and reinforcement. Reinforcement particles size used in present experimentation is less than 100µm. As received fly ash reinforcement particles are inserted into the melt. To enhance the wettability between the reinforcement and the matrix, magnesium in 1 wt. % is injected in the crucible just before the addition of particle. The composite material is manufactured in a cast iron crucible of 4 kg capacity. While manufacturing the composite, 3000 g of A356 alloy and respective wt. % of reinforcement are used. At the time of stirring at 500 rpm, the melt A356 alloy is kept at 800°C temperature for approximately 8 min.

Table 3 Microstructure findings

S.N.	Name of material	Average grain size (µm)	SDAS (µm)
1	A356	6.98	29
2	A356 – 4% fly ash	5.56	23
3	A356 – 8% fly ash	7.18	31
4	A356 – 12% fly ash	7.31	22
5	A356 – 4% Al <sub>2</sub> O <sub>3</sub>	7.78	24
6	A356 – 8% Al <sub>2</sub> O <sub>3</sub>	8.93	32
7	A356 – 12% Al <sub>2</sub> O <sub>3</sub>	6.09	22
8	A356 – 2% fly ash + 2% Al <sub>2</sub> O <sub>3</sub>	6.65	21
9	A356 – 4% fly ash + 4% Al <sub>2</sub> O <sub>3</sub>	7.33	30
10	A356 – 6% fly ash + 6% Al <sub>2</sub> O <sub>3</sub>	5.06	21

Table 4 (a) EDS of 4% fly ash reinforced composite

Element	(keV)	mass%	Error%	At%	Compound	mass%	Cation	K
O		47.07						
Al K	1.486	50.58	1.05	92.92	Al <sub>2</sub> O <sub>3</sub>	95.57	15.29	96.4625
Si K	1.739	1.64	1.84	5.80	SiO <sub>2</sub>	3.52	0.48	1.9872
Ca K	3.690	0.03	1.45	0.07	CaO	0.04	0.01	0.0709
Fe K	6.398	0.68	2.85	1.21	FeO	0.88	0.10	1.4794
Total		100.00		100.00		100.00	15.88	



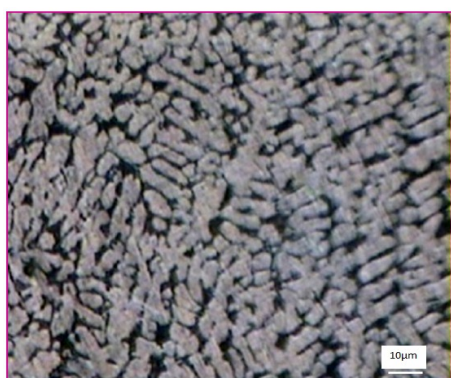
Table 4 (b) EDS of 8% fly ash reinforced composite

Element	(keV)	mass%	Error%	At%	Compound	mass%	Cation	K
O		47.17						
Al K	1.486	50.33	1.04	92.07	Al <sub>2</sub> O <sub>3</sub>	95.09	15.18	96.4180
Si K	1.739	1.97	1.82	6.93	SiO <sub>2</sub>	4.22	0.57	2.3959
Ca K	3.690	0.10	1.45	0.25	CaO	0.14	0.02	0.2483
Fe K	6.398	0.43	2.84	0.76	FeO	0.55	0.06	0.9378
Total		100.00		100.00		100.00	15.84	

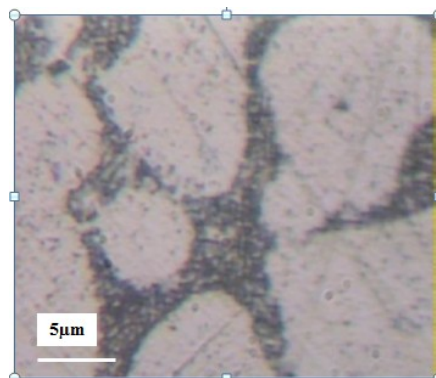
Table 4 (c) EDS of 12 % fly ash reinforced composite

Element	(keV)	mass%	Error%	At%	Compound	mass%	Cation	K
O		47.11						
Al K	1.486	49.28	1.00	89.08	Al <sub>2</sub> O <sub>3</sub>	93.10	14.88	94.5668
Si K	1.739	2.63	1.73	9.13	SiO <sub>2</sub>	5.62	0.76	3.2468
Ca K	3.690	0.11	1.39	0.26	CaO	0.15	0.02	0.2669
Fe K	6.398	0.87	2.72	1.53	FeO	1.12	0.13	1.9196
Total		100.00		100.00		100.00	15.80	

The reinforcement particles preheated at 400°C are added in the vortex generated during stirring. Turbine stirrer is used for Stirring process. Hexachloroethane tablet with 0.05 % amount is used for degassing purpose. Pre heating of cast iron mould is done at 300°C. The molten material is poured into a preheated mould and allowed to cool at room temperature. Distribution and existence of reinforcement is ensured by doing optical microscopy as shown in Figure 2 and Figure 3. To study the microstructure, specimens are prepared by cutting the cast rods. Cut specimens are belt ground and polished with emery papers of different grade. Specimens polished by emery paper are washed and cloth polished. Etching is carried and microstructure study is conceded for 100, 250 and 400 magnifications. Figure 2 (a) shows the microstructure image of A356–4% fly ash composite, Figure 2 (b) demonstrates the microstructure image of A356–4% alumina composite and Figure 2 (c) illustrates the microstructure image of A356–4% hybrid composite. The microstructural images showed that manufactured composites have refined grain size as well as secondary dendrite arm spacing. Table 3 shows results arising from microscopy. Average grain size and secondary dendrite arm spacing (SDAS) values play an important role in microstructure study. Smaller grain size always gives better properties. The stirring process done at high temperature helped in grain refinement. Smaller grain refinement and SDAS achieves better distribution of particles which helps in better mechanical properties [26]. SEM image of A356–4 % alumina and A356–12 % hybrid composite is shown in Figure 3 (a) and Figure 3 (b) respectively. The Figure 3 confirms the existence and distribution of reinforcement particles inside the A356 matrix material. Table 3 shows that all the materials have good grain refinement and virtually all the materials have an average grain size within the range of 5.06  $\mu\text{m}$  to 8.93  $\mu\text{m}$ . Moreover, SDAS values are withal lower and



Magnification 100X

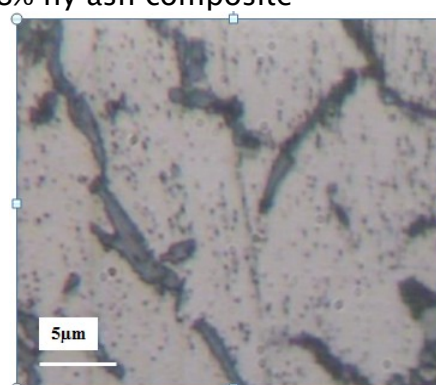


Magnification 400X

(a) Microstructure of A356-8% fly ash composite



Magnification 100X

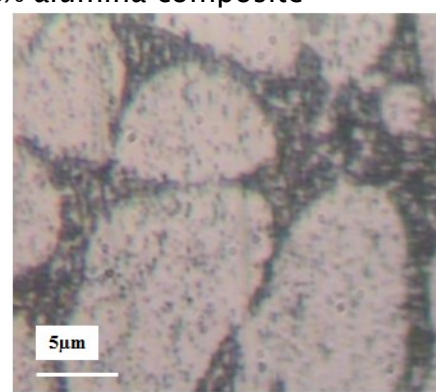


Magnification 400X

(b) Microstructure of A356-8% alumina composite



Magnification 100X



Magnification 400X

(c) Microstructure of A356-8% hybrid composite

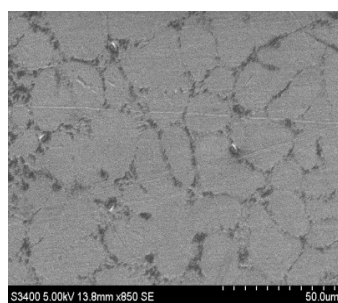
**Figure 2. Microstructure of various composites.**

within the range of 21  $\mu\text{m}$  to 32  $\mu\text{m}$  which is relevant with literature [26]. Figure 2 (a),(b) and (c) shows microstructure images of A356-4% fly ash, A356-4% alumina and A356-4% hybrid composite under 100X, 250X and 400X magnification. The microstructure of

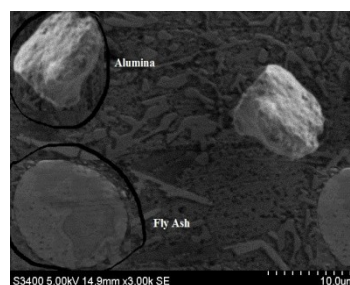
different composites shows a uniform distribution of reinforcement particles, good bonding between matrix material and reinforcement particles without any gap between them. Figure 3 (a) and (b) shows the reinforcement particles are located on grain boundaries which is relatable with Hebbar et al.[11] and Babu et.al.[23]. EDS tests on A356–fly ash manufactured composites after 4, 8 and 12 % reinforcement additions are presented in Table 4(a) to Table 4(c). The comparative study is made and it is found that the percentage of fly ash ingredients like silica, calcium oxide increases and percentage of aluminium decreases after fly ash reinforcement addition in A356 alloy. It is revealed in composite mass fraction also. Table 5 exemplifies the rise in silica percentage from 1.98%, to 3.24% after 4 to 12 % fly ash addition. Similarly, the fall in aluminium percentage from 95.46% to 94.56 % is found after 4 to 12 % fly ash addition. Table 5 clearly indicates that the composite materials are successfully manufactured and has taken the effect of reinforcement addition. The similar observations are found for other composites.

Table 5 EDS analysis of A356–fly ash reinforced composites

Composite →	4% Fly Ash			8% Fly Ash			12% Fly Ash		
Element ▼	Comp	Mass	Total	Comp	Mass	Total	Comp	Mass	Total
Aluminium/ Alumina	95.57	50.58	96.46	95.09	50.33	96.41	93.10	49.28	94.56
Silicon/ Silica	3.52	1.64	1.98	4.22	1.97	2.39	5.62	2.63	3.24



(a) SEM of A356–4 % alumina



(b) SEM of A356–12 % hybrid

Figure 3. SEM study of composite for reinforcement distribution.



## Corrosion test

The composite samples manufactured by stir casting method are tested by electrochemical method to found their corrosion behavior with the help of potentiodynamic polarization and open circuit potential (OCP) measurements. The experiments are carried out using an AC Impedance Analyzer (CHI 608c, USA) with engrained software. The corrosion testing are accomplished using a three-electrode corrosion cell set-up considering the sample as the working electrode, saturated silver/silver chloride as reference electrode, and platinum rod as counter electrode. The surfaces of the material specimen are ground with grit papers as per ASTM standard, cleaned with distilled water, dried and washed with acetone. The corrosion tests are conducted for 10 minutes at room temperature in 3.5% NaCl solution as an electrolyte. The OCP value for manufactured composites is measured. Potentiodynamic polarization measurements are also carried out. The electrolyte is replaced after each experiment. The repeatability tests are conducted and no significant difference is observed in test results.

## Results and discussion on electrochemical studies

The potentiodynamic polarization curves for the stir cast composites in 3.5% NaCl solution gives suitable information about corrosion behavior. Figure 4 to Figure 9 indicates that the composites exhibited nearly similar polarization curves. The corrosion potentials ( $E_{\text{corr}}$ ) of the manufactured composites in present study are clearly defined in the ranges of  $-0.829$  to  $-0.890\text{V}$ . With increasing applied voltage, a fairly constant region in the current density is observed as shown in Figure 4 to Figure 6 indicating the probability of the materials forming passive layers. However, it is also observed that the composites as well as the matrix alloy show a susceptibility to undergo pitting. Figure 4 (a), Figure 4 (b) and Figure 7 shows that 4 wt. % fly ash reinforced composite has the minimum thermodynamic tendency to corrode in the 3.5 wt. % NaCl solution. Similarly Figure 5, Figure 6 and Figure 7 shows that 4 wt. % alumina and 4 wt. % hybrid reinforced composites has also lesser thermodynamic tendency to corrode in NaCl solution. Figure 4 and Figure 8 indicates that 8 wt. % fly ash reinforced composite are also stable in the 3.5 wt. % NaCl. As stated by complexation corrosion theory,  $\text{Al}_2\text{O}_3$  film formed on the aluminium surface in neutral chloride medium offers good corrosion resistance., The silica in fly ash may react with Al according to Reactions(1) and generate  $\text{Al}_2\text{O}_3$  [27] which may be the reason to increase the stability of 4 wt. % fly ash reinforced composites. During the reaction, the fly ash particles progressively decompose. Also, the Si elements can form intermetallic compounds with the Al and appear as second-phase precipitates in material.



The anodic and cathodic reactions of aluminium in chloride medium make dissolution of aluminium as shown in the Reaction (2) and (3) [28].



Further the  $\text{Al}_3^+$  produced in Reaction (2) and  $\text{OH}^-$  produced in Reaction (3) generates aluminum hydroxide on aluminium surface as shown in Reaction (4)



As shown in Reaction (5), aluminium hydroxide produced on the surface of aluminium progressively converts into aluminium oxide resulting in the passive film formation on the surface of the aluminium [28].



Table 6 shows clearly that the corrosion potentials ( $E_{\text{corr}}$ ) of the composites increased with increase in fly ash content up to 8 wt. % (Figure 4). It demonstrates the stability of the composites increases with increment in fly ash content up to 8 wt. % (As corrosion potential increases to more positive values with the fly ash content). It is also observed that further increasing fly ash content (12 wt. %) susceptibility of the composite corrosion increased decreasing the corrosion potential below that of the unreinforced A356 alloy. The variation in corrosion potentials of AA2024–fly ash [23] and A356–fly ash composites is compared as shown in Table 7. It is observed from corrosion potentials ( $E_{\text{corr}}$ ) that A356 matrix and composites of A356–fly ash are found to be more stable than AA2024–fly ash for corrosion resistance. The improvement in corrosion resistance by the addition of 2-3 wt% bamboo leaf ash is also reported [28] due to the presence of silica which is the principal constituent of ash. The mixture of reinforcement inclusions and defects formed at the time of MMC fabrication decrease the susceptibility of composites to pitting by reducing the required driving force. Due to addition of magnesium in A356 alloy (7 % silicon) at the time of casting the matrix alloy and composites may contain the Al–Si rich and  $\text{Mg}_2\text{Si}$  intermetallic phases. The intermetallic phase elements oxidises and forms respective oxides such as  $\text{SiO}_2$ , FeO and MgO [27] which may have reduced the corrosion rate in fly ash reinforced composites at 4% reinforcement by reducing the microgalvanic coupling among matrix and

intermetallic phases in composites. The effect may be more prominent in A356–8 wt. % fly ash reinforced composites as they consist of more aggregates of intermetallic phases. Thus the corrosion resistance is enhanced in the case of 4 and 8 % fly ash reinforced A356 matrix composites.

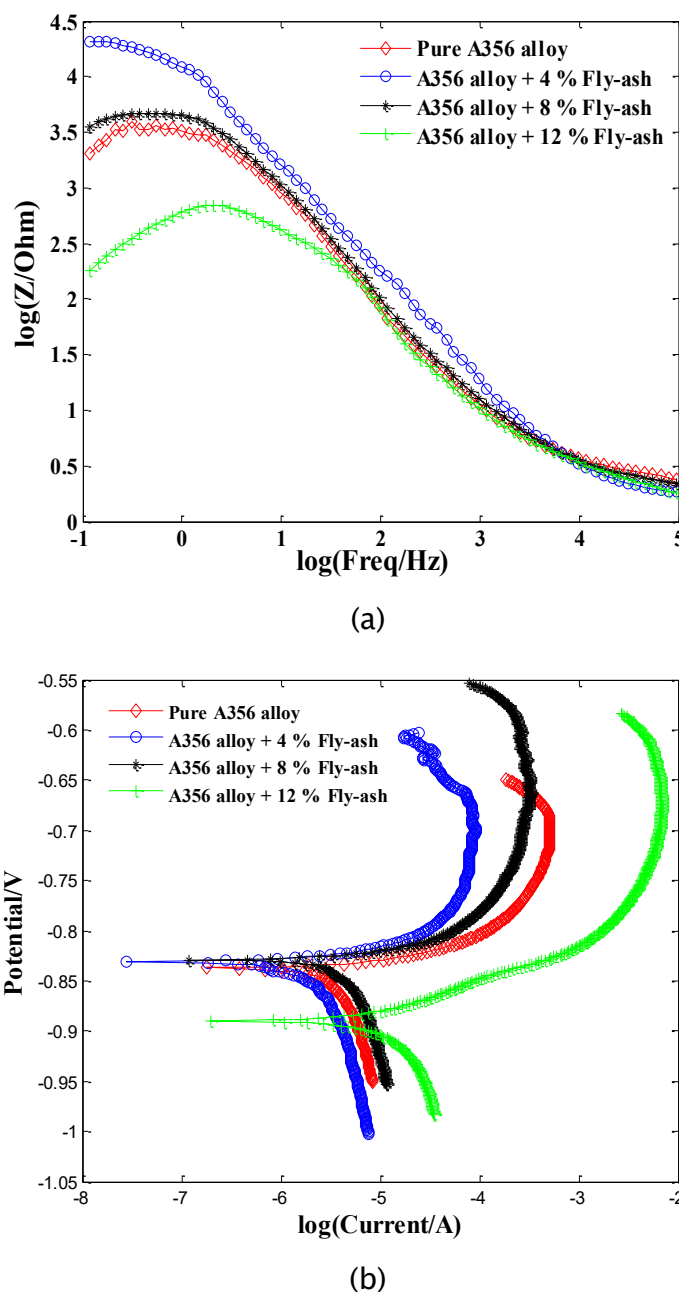
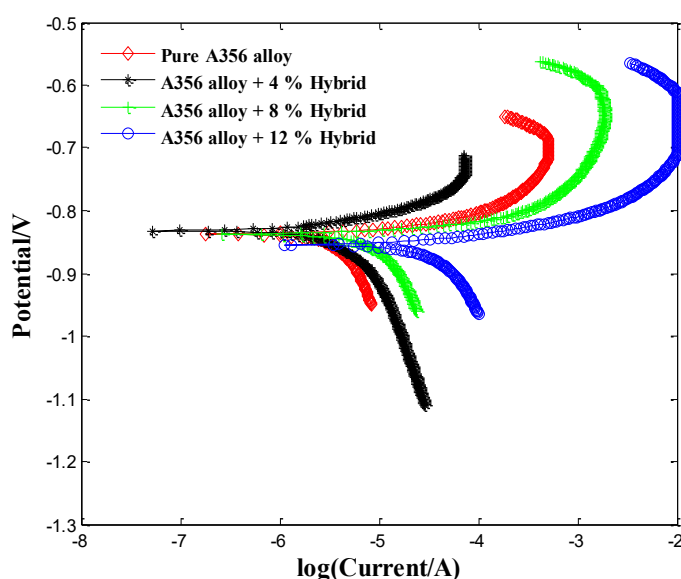


Figure 4. (a) Experimental impedance spectra for A356–fly ash composite in 3.5 wt. % NaCl solution.

(b) Potentiodynamic polarization curves for the A356–fly ash composites in 3.5%

### NaCl solution.

Correspondingly, Figure 4, Figure 5, Figure 6 and Figure 9 shows that the OCP profiles of the composites containing 12 wt. % of fly ash, alumina and hybrid are shifted to negative potential showing more thermodynamic tendency to corrode in the 3.5 wt. % NaCl solution than unreinforced A356 alloy. As reported by Murthy and Singh [29], adsorption of  $\text{Cl}^-$  ions on the aluminium surface rises and aluminium becomes sensitive to pitting corrosion. Furthermore, the adsorption of  $\text{Cl}^-$  ions on the crystal lattice of the oxide hydrates film converts corrosion potential of aluminium more negative. Corrosion potential values ( $E_{\text{corr}}$ ) increased than pure A356 matrix in case of fly ash reinforced composites up to 8 % reinforcement addition showing stability against corrosion. Nevertheless, it is detected that in case of alumina and hybrid type of reinforced composites up to 4 % reinforcement addition the composites are stable as shown in Table 6. It may be attributable to breakdown of passive film caused by exposure to a corrosive environment [30]. Moreover, it is also reported that oxide film does not gives adequate protection against aggressive chlorides anions [31].



**Figure 5 Potentiodynamic polarization curves for the A356–hybrid composites in 3.5% NaCl solution.**

In MMCs, corrosion has been recognized to be the dominant mechanism because of the physical or chemical heterogeneity such as intermetallic, dislocation, inclusion, reinforcement/matrix interface, mechanically damaged region, grain boundary, etc. where



corrosion can be favorably starts [32]. As a result of this pits originate in the matrix near the particle–matrix interface.

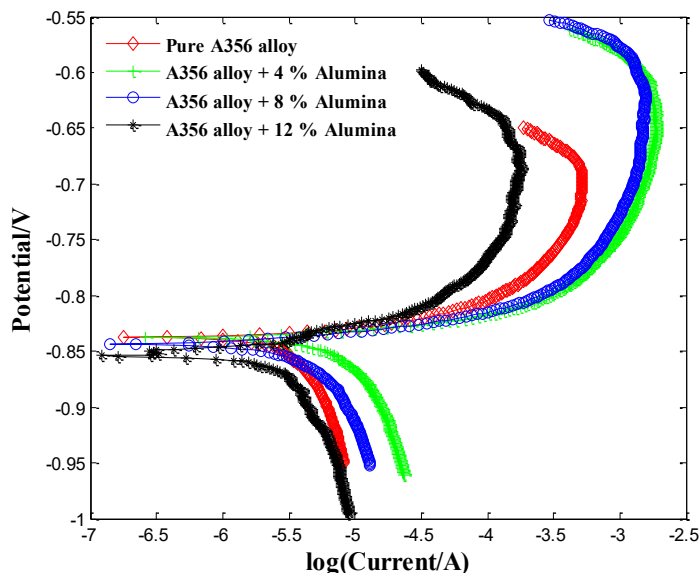


Figure 6 Potentiodynamic polarization curves for the A356–alumina composites in 3.5% NaCl solution.

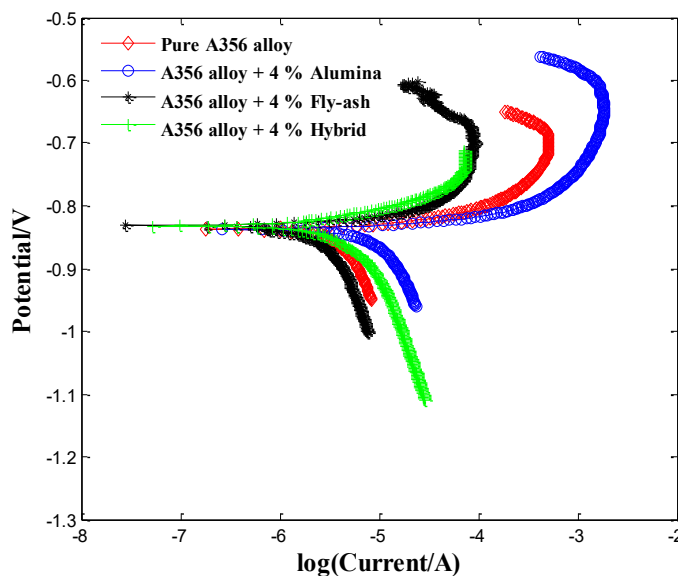
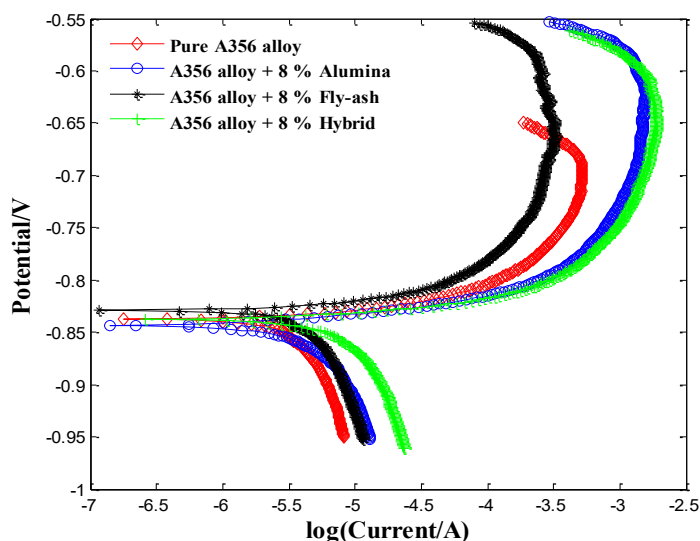
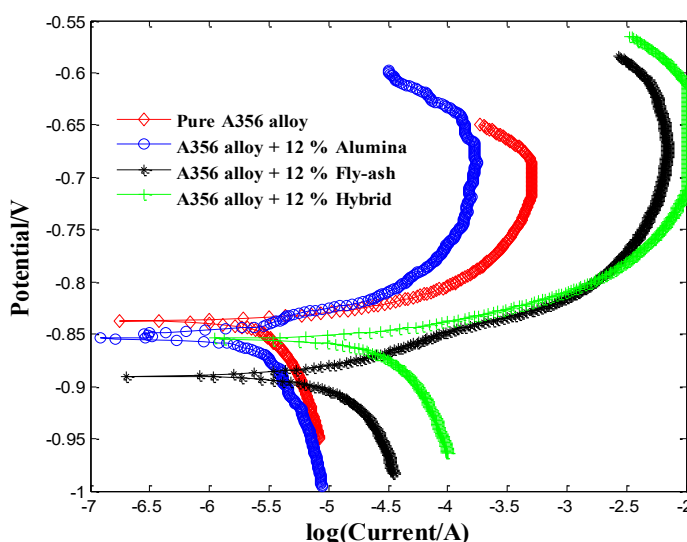


Figure 7 Potentiodynamic polarization curves for the A356–4 % fly ash, A356–4 % alumina and A356–4 % hybrid reinforced composites in 3.5% NaCl solution.



**Figure 8** Potentiodynamic polarization curves for the A356–8 % fly ash, A356–8 % alumina and A356–8 % hybrid reinforced composites in 3.5% NaCl solution.



**Figure 9** Potentiodynamic polarization curves for the A356–12 % fly ash, A356–12 % alumina and A356–12 % hybrid reinforced composites in 3.5% NaCl solution.

The SEM images confirm that dissolution of the anodic A356 alloy matrix happens at the A356matrix/ fly ash particle interfaces decreasing thermodynamic stability as shown in Figure 10. The microstructures of composite discovered a higher pitting corrosion in the composite. At 12 wt. % reinforcements, intermetallic precipitates at the interface prevent

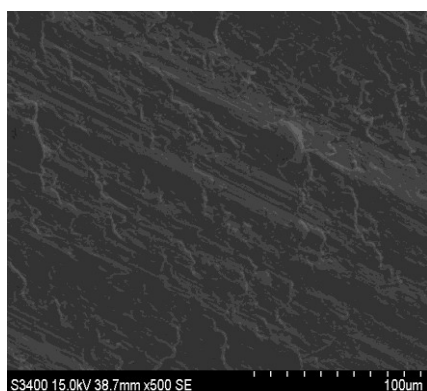
the development of a constant resistive layer of reinforcement particles across the entire surface in the MMCs.

Table 6 Effect of reinforcement addition on the corrosion potential values of composites

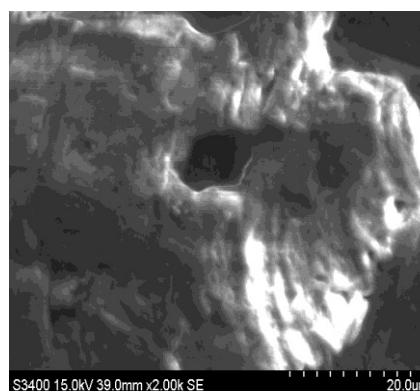
Name of material	Corrosion Potential ( $E_{\text{corr}}$ ) (mv)
Pure A356	-837
A356 – 4% fly ash	-831
A356 – 8% fly ash	-829
A356 – 12% fly ash	-890
A356 – 4% $\text{Al}_2\text{O}_3$	-838
A356 – 8% $\text{Al}_2\text{O}_3$	-843
A356 – 12% $\text{Al}_2\text{O}_3$	-854
A356 – 2% fly ash + 2% $\text{Al}_2\text{O}_3$	-832
A356 – 4% fly ash + 4% $\text{Al}_2\text{O}_3$	-838
A356 – 6% fly ash + 6% $\text{Al}_2\text{O}_3$	-854

Table 7 Comparison of  $E_{\text{corr}}$  values for fly ash reinforced composite

Material	Corrosion Potential ( $E_{\text{corr}}$ ) (mv) (Matrix material A356) [Present]	Corrosion Potential ( $E_{\text{corr}}$ ) (mv) (Matrix material AA2024) [23]
Pure	-837	-1347.4
4 % Fly Ash	-831	-1193.7
8 % Fly Ash	-829	-1251.8
12 % Fly Ash	-890	NA



(a)



(b)

Figure 10. SEM images of A356–12 % fly ash composite showing the corroded area.

The existence of reinforcement particles acts as spots to start pits. Sodium chloride solution forms pits in the aluminium. The increase in concentration of  $\text{Cl}^-$  ions starts the dissolution of aluminium in the pits and creates an additional positive charge in the pit portion [23]. It produces more migration of chlorides ions to keep electro neutrality resulting in greater concentrations of ions in pits and hydrolysis. In composites addition of higher (12 wt.%) reinforcement percentage to the matrix also produces galvanic couples favorable to corrosion. Moreover, factors influencing corrosion of the composites include porosity, high dislocation density, voids at the reinforcement/matrix interface and electrical conductivity of the reinforcements [33,34].

## CONCLUSIONS

The corrosion behaviour of A356 matrix composites containing 4, 8 and 12wt% of fly ash, alumina and hybrid as reinforcement is investigated with the help of EIS. The result analysis showed that:

1. The corrosion resistance of the A356– fly ash composites increased in 3.5% NaCl solution initially for lower reinforcement (4 and 8 wt. % reinforcement) due to  $\text{Al}_2\text{O}_3$  passive film formation on the aluminium surface. But corrosion drastically increased in 12 wt. % reinforced composites as a result of existence of more number of reinforcement particles acting as a spot for pitting corrosion.
2. Aggressive chlorides anions broke the passive film caused by exposure to a corrosive environment. Similarly, the corrosion resistance of the A356–hybrid composites also increased in 3.5% NaCl solution initially for lower reinforcement (4 wt. % reinforcement). But corrosion increased after 8 wt. % reinforcement as a result of existence of more number of reinforcement particles.
3. The A356–fly ash composites are found to be more stable for corrosion resistance as compared to A356–alumina and A356–hybrid composites at lower reinforcements.
4. The corrosion resistance of the A356– fly ash composites is found to be more superior to AA2024– fly ash composites.
5. Fly ash reinforcement addition in aluminium or its alloy have proved enhanced mechanical and wear resistance properties. Additionally, the fly ash as an industry waste can be utilized for production of low cost A356–fly ash and A356–hybrid composites at lower reinforcement manufactured by conventional stir casting method for corrosion resistance application.



## References

1. D. S. Prasad, C. Shoba and N. Ramanaiah, J. Mater. Res. Technol., 3 (2014): p.79.
2. S. Zhang and F. Wang, J. Mater. Process. Technol., 182 (2007): p.122.
3. R. K. Uyyuru, M.K. Surappa and S. Brusethaug, Tribol. Int. 40 (2007): p.365.
4. R.N. Rao and S. Das, Mater. Des., 32 (2011): p.1066.
5. M K Surappa, Sadhana, 28 (2003): p. 319.
6. P. K. Rohatgi, B. F. Schultz, A. Daoud and W.W.Zhang, Tribol. Int., 43 (2010): p. 455.
7. T.P.D. Rajan, 2007, Composites Science and Technology p. 70.
8. P.K. Rohatgi, JOM 46 (1994): p.55.
9. Sudarshan and M. K. Surappa, Mater. Sci. Eng. A, 480 (2008): p.117.
10. S. Zahi and A.R. Daud, Mater. Des., 32 (2011): p.1337.
11. H.C. Anilkumar, H.S. Hebbar and K.S. Ravishankar, International Journal of Mechanical and Materials Engineering, 6 (2011): p.41.
12. M. Ramachandra, K. Radhakrishna, Wear, 262 (2007): p.1450.
13. S. Amirkhanlou, B. Niroumand, Mater. Des., 32 (2011): p.1895.
14. J. Hashim, J. Mater. Process. Technol, 93 (1999): p.1.
15. J. Hashim, J. Mater. Process. Technol., 119 (2001): p.324.
16. S. Suresha and B. K. Sridhara, Compos. Sci. Technol., 70 (2010): p.1652.
17. R. E. Lozano, C. Gutierrez, M. A. Pech, Canul and M. I. Pech-Canul, Waste Manage, 28 (2008): p.389.
18. M. B. Mahagundappa and H.K. Shivanand, Wear 262 (2007): p.759.
19. L.A. Dobrzanski, M. Kremzer and M. Adamiak. Journal of Achievements in Materials and Manufacturing Engineering, 42 (2010): p. 26.

20. B. Bobic, S. Mitrovic, M. Babic and I. Bobic., Tribology in industry, 32 (2010): p.3.
21. K. K. Alaneme and M. O. Bodunrin, Journal of Minerals and Materials Characterisation and Engineering, 10 (2011): p.1153.
22. M. S. Turhal and T. Savaskan, J. Mater. Sci., 38 (2003): p.2639.
23. R. J. Babu, V. D. Rao, N. I. Murthy and N. R. M. R Bhargava, J. Compos. Mater., 46 (2011): p.1393.
24. K. K. Alaneme:, Leonardo Journal of science, 18 (2011): p.55.
25. S. G. Kulkarni, J. V. Meghnani and A. Lal, Procedia Mater. Sci., 5(2014): p. 746.
26. L. A. Dobrzański, R. Maniara, J. H. Sokolowski, Archives of Materials Science and Engineering, 28 (2007): p.105.
27. R. Q. Guo and P. K. Rohatgi, Metall. Mater. Trans. B, 29 (1998): p.519.
28. K. K. Alaneme, P. A. Olubambi, A. S. Afolabi and M. O. Bodurin, Int. J. Electrochem. Sci, 9 (2014): p. 5663.
29. H. C. Ananda Murthy and S. K. Singh, Adv. Mater. Lett. 6(2015): p. 633.
30. K. K. Alaneme, P. A. Olubambi, J Mater Res Technol, 2 (2013): p.1884.
31. R. Rosliza, W.B. Wan Nik, Curr. Appl Phys., 10 (2010): p.221.
32. A. J. Dolata, M. Dyzia, W. Walke, Solid State Phenomena, 191(2012): p.81.
33. A. J. Trowsdale, B. Noble, S. J. Harris, I.S.R. Gibbins G.E. Thompson and G.C. Wood, Corros. Sci., 38 (1996): p.177.
34. R. L. Deuis, L. Green, C. Subramanian and Yellup, Corrosion, 53 (1997): p.880.